Research Journal of Applied Sciences, Engineering and Technology 12(3): 355-360, 2016
DOI: 10.19026/rjaset.12.2343
ISSN: 2040-7459; e-ISSN: 2040-7467

Submitted: August 28, 2015 Accepted: October 11, 2015 Published: February 05, 2016

**Research Article**

# Bright Lesion Detection in Color Fundus Images Based on Texture Features

V. Ratna Bhargavi, Ranjan K. Senapati, Ganesh Methra and Sujitha Kandanulu
Department of Electronics and Communication Engineering, K L University, Vaddeswaram, Guntur-522502, Andhra Pradesh, India

**Abstract:** In this study a computer aided screening system for the detection of bright lesions or exudates using color fundus images is proposed. The proposed screening system is used to identify the suspicious regions for bright lesions. A texture feature extraction method is also demonstrated to describe the characteristics of region of interest. In final stage the normal and abnormal images are classified using Support vector machine classifier. Our proposed system obtained the effective detection performance compared to some of the state-of-art methods.

**Keywords:** Classification, computer aided screening, diabetic retinopathy, feature extraction, segmentation

## INTRODUCTION

Diabetic Retinopathy (DR) is the leading cause of blindness and it is the diabetic eye disease. According to International Diabetes Federation (IDF) (2013) now people are having diabetes is about 387 million worldwide and it will be increased to 592 million by 2035. IDF declared that 52% of Indians are not knowing about diabetes that they are suffering with high blood sugar. In rural India around 34 million people effected with diabetes compared to urban Indians around 28 million people (International Diabetes Federation (IDF), 2013).

Due to the damage of the vessels of the retina this disease will occur. Blood vessels may swell and fluid leakage will happen. So that pathologies will occur. The pathologies in the early stage should be recognized to prevent blindness. For this purpose Computer Aided Detection (CADe) system will help as a second opinion for early diagnosis. Now some of diabeticians are also using fundus camera to analyze the color fundus images by screening diabetic retinopathy for lesions. This avoids vision loss in diabetes attacked patients. A physician and CADe system will do the same task, i.e., the identification of lesions from fundus images. But system software tool will identify and mark the suspicious regions for physician review. To raise the accuracy of diagnosis, CADe systems are developed to help the physicians or diabeticians as assistants for the recognition of lesions.

Bright lesions or exudates are the pathologies which appear bright yellow or white color with varying sizes and shapes. So the yellow color patches should be identified in the early stage to prevent the number of blindness. A numerous techniques are developed for pathologies detection. Exudates are one of the earliest signs of diabetic retinopathy. Sinthanayothin *et al*. (1999) proposed Recursive Region-Growing Segmentation (RRGS) and thresholding algorithms. This give rise to sensitivity and specificity of 88.5 and 99.7% respectively. Jayakumari and Santhanam (2007) implemented contextual clustering and they used features such as convex area, solidity, orientation for classification. They reported sensitivity and specificity of 93.4, 80% respectively. Welfer *et al*. (2010) proposed morphological and thresholding techniques for lesion detection and they obtained sensitivity and specificity of 70.5 and 98.8% respectively. Lin and Bing-Kun (2012) proposed an automated technique for exudates segmentation and it is based on Fuzzy c-means clustering algorithm. The obtained sensitivity and specificity are 84.8 and 87.5% respectively. Wisaeng *et al*. (2015) proposed the moving average histogram model and exact location of exudates are marked by sobel and Otsu's thresholding. The obtained Area Under Curve (AUC) is 93.69%. Esmaeli *et al*. (2012) recently proposed exudates detection by using digital curvelet transform and they used to change the coefficients of curvelets and level segmentation. The obtained sensitivity and specificity are 98.4 and 90.1%, respectively. Rocha *et al*. (2012) proposed lesions identification in visual words and the AUC is 95.3%. Agurto *et al*. (2010) proposed multi-scale optimization approach for lesion detection. It uses AM-FM representations, where partial least square method has applied for classification in normal and abnormal images. Recently, Giancardo *et al*. (2012) proposed bright lesion detection based on the probability maps, color and wavelet analysis. The AUC obtained is around 0.88 to 0.94. Pires *et al*. (2013) proposed soft

**Corresponding Author:** V. Ratna Bhargavi, Department of Electronics and Communication Engineering, K L University, Vaddeswaram, Guntur-522502, Andhra Pradesh, India

assignment coding/max pooling for exudates detection; and for feature extraction Speeded Up Robust Feature extraction (SURF) algorithm is implemented. The reported AUC is 93.4%. Harangi and Hajdu (2014) proposed multiple active contour technique for lesion detection and region wise classification is done for distinguishing the normal and abnormal images. The sensitivity, specificity and AUC are 92.1, 68.4 and 0.82 respectively. For the detection of lesions, motion patterns are created for region of interest in color fundus images by Deepak and Sivaswamy (2012). For feature extraction Radon transform is used. The sensitivity and specificity are reported to be 100 and 74%, respectively. Pachiyappan *et al*. (2012) proposed morphological dilation, closing, filling and threshold criteria for bright lesion detection. This give rise to an accuracy about 97.7%. Roychowdhury *et al*. (2014) proposed a novel technique based on maximum solidity and minimum intensity for lesion detection. Lesion classified based on hierarchical classification. The obtained sensitivity and specificity are 100% and 53.16% respectively. Ravishankar *et al*. (2009) proposed localization of lesions, based on color properties, intensity variations and morphological operations. They obtained sensitivity and specificity are 95.7 and 94.2% respectively. Van Grinsven *et al*. (2013) proposed a bag of visual words approach to characterize the fundus image. They implemented decomposition of image as patches. From each image patch, various features are extracted and classification was done based on weighed nearest neighbor method. The resulted AUC is 0.90.

In this study our objective is to made use novel combination of the existing techniques in order to achieve better sensitivity, specificity and accuracy than the previously used techniques. In our proposed method, the bilateral filtering step is applied as a preprocessing step, because fundus images in datasets are having noise and they are poorly illuminated. Contrast enhancement is done to increase the contrast between foreground with exudates and background elements like Optic Disk (OD) and vessels. The anatomical structures of OD and vessels are extracted and eliminated for visualization of lesions clearly. The remaining foreground lesions are segmented. In order to characterize the segmented lesions, texture features are calculated. Finally Support Vector Machine classifier (SVM) is used to distinguish the lesions and non-lesions images.

## PROPOSED METHOD

The proposed method is a four stage CADe system for lesion detection in color fundus images. The first stage comprises pre-processing and the next stage is segmentation of anatomical structures and pathological parts. The stage three is feature extraction and the final stage is classification. Figure 1 shows the block diagram of proposed technique and the following sections will give detailed explanation about each method.

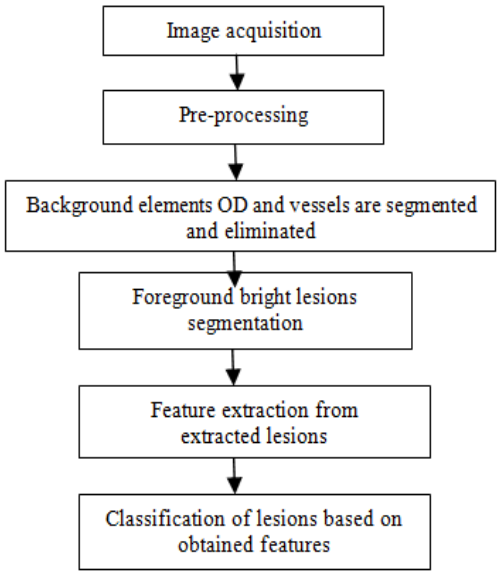


Fig. 1: Block diagram of proposed CADe system for lesion detection

**Image pre-processing:** The pre-processing of fundus images reduces or removes the effects of noises, vessel parts and some patches visible like lesions (Fig. 2a). All images using here are preprocessed because images in datasets are often noisy and they are having poor illumination. First we extract green channel $I_g$ so that exudates appear brighter in this channel compared to other channels (Fig. 2b). Now histogram equalization and contrast enhancement are applied on $I_g$. Then, contrast between foreground and background structures is increased and resulting $I_{hist}$ shown in Fig. 2c. In order to remove unwanted some visible spots, noise, lines, obstacles, Bilateral Filter (BF) (Petschnigg *et al*., 2004) is used. Because it smoothens flat surfaces while preserving sharp edges in image by having same pixels placed in every neighborhood $I_{bf.}$ This is shown in Fig. 2d.

**Segmentation of opticdisk and vessels:** In this stage first we extract the Optic Disk (OD) and main vessel parts. Then, these structures are masked out because there is higher order similarity in between bright lesions, OD vessel structures. Generally, OD and vessels are recognized as lesions by mistake. The OD structure is segmented using image dilation by having disk structuring element (10, 4). The resulting binary image with OD is shown in Fig. 2e. The multi-scale hessian matrix shown in (1) is used to find the tubular structure. We have extracted the vessel structures using the same multi-scale hessian matrix:

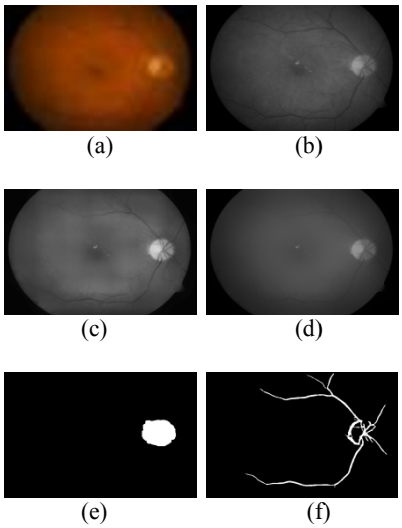

Fig. 2: (a): Color fundus image; (b): Green channel extracted image; (c): Histogram equalized image; (d): Bilateral filter applied image; (e): Optic disk extracted image; (f): Vessel extracted image based on Hessian matrix transform

$$H = \begin{bmatrix} \partial^2 I/\partial x^2 & \partial^2 I/\partial x \partial y \\ \partial^2 I/\partial y \partial x & \partial^2 I/\partial y^2 \end{bmatrix} \quad (1)$$

where, I is the pre-processed image. Second order partial derivative for the image I is done. We can have eigen values with following conditions for an ideal tubular structure:

$$|\lambda_1| \approx 0$$
$$|\lambda_1| \ll |\lambda_2|$$

The vessel function is given by V(l):

$$V(l)=(|\lambda_1|/2).e^{|b-|\lambda_1|/\sqrt{\lambda_1+\lambda_2}|} +(|\lambda_2|/2).e^{|(|\lambda_2|/\sqrt{\lambda_1+\lambda_2})-b|}$$

V(l) is a function and its value gives the tubular structure for every pixel. The maximum function value V(l) corresponds to pixel value that stands for scale. The main vessel is having a large scale property. The extracted image $I_{vl}$ shown in Fig. 2f.

**Lesion detection by removing opticdisk and vessels:** Now it is essential to remove the optic disk and main vessel parts. We are having the binary images with extracted optic disk $I_{OD}$ and vessel structures $I_{vl}$ shown in Fig. 2e and f. The elements of binary image with optic disk and the elements of binary image with vessel are subtracted from unity. Now in the resultant images, each element is multiplied with the illumination corrected image elements presented in (2) and (3). Then both the structures i.e., optic disk and main vessels are masked out. This is shown in Fig. 3a:

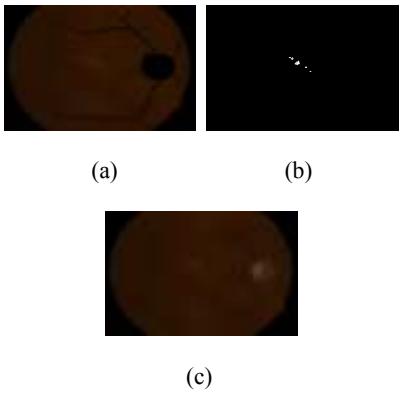

Fig. 3: (a): Masked out optic disk and vessels; (b): Thresholded image; (c): Lesion segmented image

Table 1: Features extracted from ROI

| No. | Feature |
|---|---|
| 1 | Total number of pixels in the ROI |
| 2 | Distance from centre of OD |
| 3 | Distance from vascular region |
| 4 | Minimum pixel intensity in Ig |
| 5 | Maximum pixel intensity in Ig |
| 6 | Mean pixel intensity in Ig |
| 7 | Skewness of ROI |
| 8 | Entropy of ROI |
| 9 | Standard deviation of ROI |
| 10 | Correlation coefficient in ROI block |
| 11 | Minimum correlation coefficient in ROI block |
| 12 | Maximum correlation coefficient in ROI block |
| 13 | Mean of pixel intensities in ROI block |
| 14 | Distance around the detected ROI |
| 15 | Variance of pixels for the detected ROI |
| 16 | Anisotropy for detected ROI |
| 17 | Maximum pixel intensity in ROI of $I_{le}$ |
| 18 | Minimum pixel intensity in ROI of $I_{le}$ |
| 19 | Sum of pixel intensities in ROI block of $I_{le}$ |
| 20 | Distance from macular region in $I_{le}$ |

$$I_{M(OD)} = I_{illu} * \left(1 - ele(I_{OD})\right) \quad (2)$$

$$I_{M(V)} = I_{illu} * \left(1 - ele(I_{vl})\right) \quad (3)$$

After the masking of the optic disk and main vessel structures, lesion parts will be segmented by thresholding based on histogram. Canny (1986) is applied to find the borders of the lesions based on thresholded image which contains exudates (Fig. 3b). The contours of yellow color exudates are drawn in the illumination corrected fundus image based on intensity pixel values of thresholded image. This results in $I_{le}$ shown in Fig. 3c.

**Feature extraction from segmented lesions:** After the detection of suspicious regions of lesion parts, the feature extraction is done to characterize the lesions shown in Fig. 3c. Now we will findout the detected patches that are lesions or non lesions. The extracted features from the detected suspicious regions are shown in Table 1. In the detected suspicious regions we can consider 2×2 or 4×4 blocks. Mostly non-correlated

Table 2: Calculated feature values

| Feature values of detected ROIs of abnormal images | Feature values of detected ROIs of normal images |
|---|---|
| 0.087 | 0.473 |
| 0.038 | 0.238 |
| 16 | 0.309 |
| 282 | 0.225 |
| 0.120 | 0.421 |
| 97 | 6 |
| 0.552 | 0.510 |
| 8.552 | 0.188 |
| 0.340 | 204 |
| 0.558 | 0.351 |
| 1.071 | 0.062 |
| 0.067 | 0.149 |
| 0.312 | 0.045 |
| 0.0227 | 0.084 |
| 0.175 | 0.287 |
| 0.153 | 0.270 |
| 0.097 | 5.396 |
| 0.028 | 88 |
| 0.164 | 0.247 |
| 0.107 | 0.126 |

feature values for normal and abnormal suspicious regions are shown in Table 2.

**Classification:** We have detected the structures with foreground and background and segmented the suspicious lesion regions. However, it is essential to classify whether the detected pathologies are true exudates or not. There are many methods available for the classification of data. In our study, we made use of Support Vector Machine (SVM) classifier which is efficient for separating two different types of datasets. The SVM classifier uses a hyper plane to separate two datasets. The features are extracted from the segmented regions for lesion classification. Now by having the feature vectors f1 and f2 from suspicious regions of normal and abnormal images, we can train the classifier assigning class labels as y = +1 or -1. During the testing of the classifier one feature vector $f^*$ is adopted and it is tested by having the feature values. Finally, it will assign which class it belongs to i.e., whether +1 or -1.

## EXPERIMENTAL RESULTS

**Dataset:** The proposed CADe system is trained and tested by adopting two publicly available datasets for normal and diseased patients. DIARETDB1 (Kauppi *et al*., 2007) dataset is having total 89 images with 50° field of view. These images are separated into two groups for training and testing. MESSIDOR (Messidor, 2010) dataset contains total 1200 images with 45° field of view. We have implemented our CAD screening system on these images.

The statistical measures used for analyzing the performance of CAD screening system defined in terms of True Positives (TP), False Positives (FP), True Negatives (TN), False Negatives (FN):

Sensitivity (sen) = TP/(TP+FN)
Specificity (spe) = TN/(TN+FP)
Accuracy (acc) = (sen+spe)/2

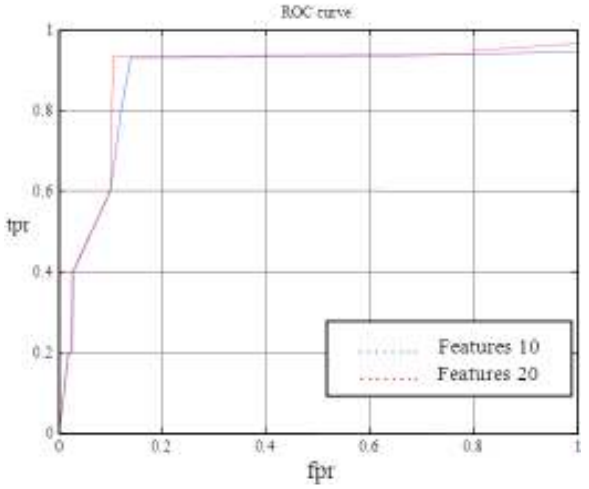


Fig. 4: ROC curve for proposed system

Table 3: Feature values selected in stepwise for classification

| Selected number of features | Sensitivity (%) | Specificity (%) | Accuracy (%) |
|---|---|---|---|
| 05 | 95.03 | 94.67 | 94.85 |
| 10 | 95 | 90.1 | 92.55 |
| 15 | 95.03 | 100 | 95.32 |
| 20 | 100 | 94.6 | 96.66 |

Table 4: Comparison of performance of previous work done (%)

| Technique | Year | Accuracy (%) |
|---|---|---|
| Sopharak *et al*. | 2008 | 89.75 |
| Sánchez *et al*. | 2009 | 88.1 |
| Pan and Bring-Kun | 2012 | 86.15 |
| Esmaeli *et al*. | 2012 | 94.25 |
| Rocha *et al*. | 2012 | 95.3 |
| Giancardo *et al*. | 2012 | 94.1 |
| Pires *et al*. | 2013 | 93.4 |
| Harangi and Hajdu | 2014 | 82.2 |
| Roychowdhury *et al*. | 2014 | 95.35 |
| Proposed method | 2015 | 96.66 |

where,

TP = Number of abnormal images correctly identified as abnormal
TN = Number of normal images correctly identified as normal
FP = Number of normal images incorrectly identified as abnormal
FN = Number of abnormal images incorrectly identified as normal

To know the diagnosis performance we have to measure the sen, spe and acc parameters. Figure 4 shows the Receiver Operating Character (ROC) curve. The graph in Fig. 4 has false positive rate or specificity on x-axis and true positive rate or sensitivity on y-axis. If an ROC curve shows AUC = 1, then it is perfect diagnosis, otherwise, if it shows 0.5, then it is worst case. In the proposed work have achieved AUC = 0.966. The measure of accuracy is proportional to the AUC.

**Analysis of classifier:** In this proposed system the used classifier is SVM. SVM is implemented in two datasets

for classification of lesions and non lesions feature values which are shown in Table 2. By analyzing classifier, the false positives are got very less and the TPs obtained are more than half of feature values taken. It is around 66.6%. Around 20 features are calculated and in stepwise (at a step of 5) features are considered for classification. The accuracy results are tabulated in Table 3. Finally our proposed system is compared with previous work done by several researchers on exudates detection. Accuracies of previous techniques are compared with proposed method and Table 4.

## CONCLUSION

The proposed CADe system is a four stage detection system. Here around 20 features are obtainedfrom lesion and non-lesion regions where feature values are calculated for classification. The AUC obtained is 0.966 and it out perform the methods proposed in the literature. So, our screening system can be able to identify the lesions and it can be a better assistant for a diabetician or physician. In our work, 20 features show the satisfactory performance by segmenting the lesion areas. Future research direction is to implement a combination of classifiers which is expected to give better accuracy. Further, we would like to perform proposed method for other lesions like cottonwool spots, Microaneurysms and Haemorrahages.

## REFERENCES


Agurto, C., V. Murray, E. Barriga, S. Murillo, M. Pattichis, H. Davis, S. Russell, M. Abramoff and P. Soliz, 2010. Multiscale AM-FM methods for diabetic retinopathy lesion detection. IEEE T. Med. Imaging, 29(2): 502-512.

Canny, J., 1986. Computational approach to edge detection. IEEE T. Pattern Anal., 8(6): 679-698.

Deepak, K.S. and J. Sivaswamy, 2012. Automatic assessment of macular edema from color retinal images. IEEE T. Med. Imaging, 31(3): 766-776.

Esmaeli, M., H. Rabbani, A.M. Dehnavi and A. Dehgani, 2012. Automatic detection of exudates and optic disk in retinal images using curvelet transform. IET Image Process., 6(7): 1-9.

Giancardo, L., F. Meriaudeau, T.P. Karnowski, Y. Li, S. Garg *et al*., 2012. Exudate-based diabetic macular edema detection in fundus images using publicly available datasets. Med. Image Anal., 16: 216-226.

Harangi, B. and A. Hajdu, 2014. Automatic exudates detection by fusing multiple active contours and region wise classification. Comput. Biol. Med., 54: 156-171.

International Diabetes Federation (IDF), 2013. Public Health Foundation of India. Data from the 2013 Fact Sheet Diabetes in India-Fact Sheet. Retrieved form: http://www.cadiresearch.org/topic/diabetes-indians/diabetes-urban-india.

Jayakumari, C. and T. Santhanam, 2007. Detection of hard exudates for diabetic retinopathy using contextual clustering and fuzzy art neural network. Asian J. Inform. Technol., 8: 842-846.

Kauppi, T., V. Kalesnykiene, J.K. Kmrinen, L. Lensu, I. Sorr, A. Raninen, R. Voutilainen, H. Uusitalo, H. Kälviäinen and J. Pietilä, 2007. Diaretdb1 diabetic retinopathy database and evaluation protocol. Proceeding of the 11th Conference on Medical Image Understanding and Analysis, pp: 61-65.

Lin, P. and Z. Bing-Kun, 2012. An effective approach to detect hard exudates in color retinal image. In: Qian, Z. and *et al*. (Eds.): Recent Advances in CSIE, 2011. LNEE 124, Springer-Verlag, Berlin, Heidelberg, pp: 541-546.

Messidor, 2010. Methods to Evaluate Segmentation and Indexing Techniques in the Field of Retinal Ophthalmology. Retrieved from: http://messidor.crihan.fr/download-en.php. (Accessed on: Sep. 23, 2011)

Pachiyappan, A., U.N. Das, T.V.S.P. Murthy and R. Tatavarti, 2012. Automated diagnosis of diabetic retinopathy and glaucoma using fundus and OCT images. Lipids Health Dis., 11: 73.

Petschnigg, G., R. Szeliski, M. Agrawala, M. Cohen, H. Hoppe and K. Toyama, 2004. Digital photography with flash and no-flash image pairs. ACM T. Graphic., 23(3): 664-672.

Pires, R., H.F. Jelinek, J. Wainer and S. Goldensteindo, E. Valle and A. Rocha, 2013. Assessing the need for referral in automatic diabetic retinopathy detection. IEEE T. Bio-Med. Eng., 60(12): 3391-3398.

Ravishankar, S., A. Jain and A. Mittal, 2009. Automated feature extraction for early detection of diabetic retinopathy in Fundus images. Proceeding of the IEEE Conference on Computer Vision and Pattern Recognition (CVPR, 2009), pp: 210-217.

Rocha, A., T. Carvalho, H. Jelinek, S. Goldenstein and J. Wainer, 2012. Points of interest and visual dictionaries for automatic retinal lesion detection. IEEE T. Bio-Med. Eng., 59(8): 2244-2253.

Roychowdhury, S., D.D. Keshabparhi and K.K. Parhi, 2014. DREAM: Diabetic retinopathy analysis using machine learning. IEEE J. Bio-Med. Health Inform., 18(5): 1717-1728.

Sánchez, C.I., R. Hornero, M.I. López, M. Aboy, J. Poza and D. Abásolo, 2009. A novel automatic image processing algorithm for detection of hard exudates based on retinal image analysis. Med. Eng. Phys., 30(3): 350-357.

Sinthanayothin, C., J. Boyce, H. Cook and T. Williamson, 1999. Automated localisation of the optic disc, fovea and retinal blood vessels from digital colour fundus images. Brit. J. Ophthalmol., 83(8): 902-10.

Sopharak, A., B. Uyyanonvara, S. Barman and T.H. Williamson, 2008. Automatic detection of diabetic retinopathy exudates from non-dilated retinalimages using mathematical morphology methods. Comput. Med. Imag. Grap., 32(8): 720-727.

Van Grinsven, M.J.J.P., A. Chakravartyy, J. Sivaswamy, T. Theelen, B. van Ginneken and C.I. Sánchez, 2013. A bag of words approach for discriminating between retinal images containing exudates or drusen. Proceeding of the IEEE 10th International Symposium on Biomedical Imaging. San Francisco, CA, pp: 1444-1447.

Welfer, D., J. Scharcanski and D.R. Marinho, 2010. A coarse-to-fine strategy for automatically detecting exudates in color eye fundus images. Comput. Med. Imag. Grap., 34(3): 228-235.

Wisaeng, K., N. Hiransakolwong and E. Pothiruk, 2015. Automatic detection of exudates in retinal images based on thresholding moving average models. Biophysics, 60(2): 288-297.